

A DIFFERENTIAL QUADRATURE FINITE ELEMENT METHOD

YUFENG XING*, BO LIU and GUANG LIU

*The Solid Mechanics Research Center
Beijing University of Aeronautics and Astronautics
Beijing 100191, China
xingyf@buaa.edu.cn*

Received 25 June 2009
Accepted 12 October 2009

This paper studies the differential quadrature finite element method (DQFEM) systematically, as a combination of differential quadrature method (DQM) and standard finite element method (FEM), and formulates one- to three-dimensional (1-D to 3-D) element matrices of DQFEM. It is shown that the mass matrices of C^0 finite element in DQFEM are diagonal, which can reduce the computational cost for dynamic problems. The Lagrange polynomials are used as the trial functions for both C^0 and C^1 differential quadrature finite elements (DQFE) with regular and/or irregular shapes, this unifies the selection of trial functions of FEM. The DQFE matrices are simply computed by algebraic operations of the given weighting coefficient matrices of the differential quadrature (DQ) rules and Gauss-Lobatto quadrature rules, which greatly simplifies the constructions of higher order finite elements. The inter-element compatibility requirements for problems with C^1 continuity are implemented through modifying the nodal parameters using DQ rules. The reformulated DQ rules for curvilinear quadrilateral domain and its implementation are also presented due to the requirements of application. Numerical comparison studies of 2-D and 3-D static and dynamic problems demonstrate the high accuracy and rapid convergence of the DQFEM.

Keywords: Differential quadrature method; finite element method; free vibration; bending.

1. Introduction

The finite element method (FEM) is a powerful tool for the numerical solution of a wide range of engineering problems. In conventional FEM, the low order schemes are generally used and the accuracy is improved through mesh refinement, this approach is viewed as the h -version FEM. The p -version FEM employs a fixed mesh and convergence is sought by increasing the degrees of element. The hybrid h - p version FEM effectively marries the previous two concepts, whose convergence is sought by simultaneously refining the mesh and increasing the element degrees [Bardell, 1996]. The theory and computational advantages of adaptive p - and hp -versions for solving problems of mathematical physics have been well documented

*Corresponding author.

[Babuska *et al.*, 1981; Oden and Demkowicz, 1991; Shephard *et al.*, 1997]. Many studies have focused on the development of optimal p - and hp -adaptive strategies and their efficient implementations [Campion *et al.*, 1996; Demkowicz *et al.*, 1989; Zhong and He, 1998]. Issues associated with element-matrix construction can be summarized as

- (1) Efficient construction of the shape functions satisfying the C^0 and/or C^1 continuity requirements.
- (2) Efficient and effective evaluations of element matrices and vectors.
- (3) Accounting for geometric approximations of elements that often cover large portions of the domain.

The efficient construction of shape functions satisfying the C^0 continuity is possible and seems to be simple for both p - and hp -versions [Shephard *et al.*, 1997], but the construction of shape functions satisfying the C^1 continuity is difficult for displacement-based finite element formulation [Duan *et al.*, 1999; Rong and Lu, 2003]. The geometry mapping for the p - and hp -version can be achieved through both the serendipity family interpolations and the blending function method [Campion and Jarvis, 1996], thus we focus on the first two issues for efficiently constructing FEM formulation satisfying the C^0 and/or C^1 continuity requirements in present study.

Analytical calculation of derivatives in the h -version is possible and usually straightforward; nevertheless, explicit differentiation is extremely complicated or even impossible in the p - and hp -versions. As a result, numerical differentiation has to be used, but which increases the computational cost [Campion and Jarvis, 1996]. An alternative method of deriving the FEM matrices is to combine the finite difference analogue of derivatives with numerical integral methods to discretize the energy functional. This idea was originated by Houbolt [1958], and further developed by Griffin and Varga [1963], Bushnell [1973], and Brush and Almroth [1975]. As the approach is based on the minimum potential energy principle, it was called the finite difference energy method (FDEM). Bushnell [1973] reported that FDEM tended to exhibit superior performance normally and required less computational time to form the global matrices than the finite element models. However, during the further applications of the FDEM [Atkatsch *et al.*, 1980; Satyamurthy *et al.*, 1980; Singh and Dey, 1990], it was found that it is difficult to calculate the finite difference analogue of derivatives on the solution domain boundary and on an irregular domain. Although the isoparametric mapping technique of the FEM was incorporated into FDEM to cope with irregular geometry [Barve and Dey, 1990; Fielding *et al.*, 1997], the lack of geometric flexibility of the conventional finite difference approximation holds back the further development of the FDEM. Consequently, it has lain virtually dormant thus far.

During the last three decades, the differential quadrature method (DQM) gradually emerges as an efficient and accurate numerical method, and has made noticeable success over the last two decades [Bellman and Casti, 1971; Bert *et al.*, 1988; Bert

and Malik, 1996; Shu, 2000]. The essence of DQM is to approximate the partial derivatives of a field variable at a discrete point by a weighted linear sum of the field variable along the line that passes through that point. Although it is analogous to the finite difference method (FDM), it is more flexible in selection of nodes, and more accurate in acquiring high approximation accuracy as compared to the conventional FDM. The late significant development of the DQM has motivated an interest in the combination of the DQM with a variational formulation. Striz *et al.* [1995] took an initiative and developed the hybrid quadrature element method (QEM) for two-dimensional plane stress and plate bending problems, and plate free vibration problems [Striz *et al.*, 1997]. The hybrid QEM essentially consists of a collocation method in conjunction with a Galerkin finite element technique to combine the high accuracy of DQM with the generality of FEM. This results in superior accuracy with fewer degrees of freedom than conventional FEM and FDM. However, the hybrid QEM needs shape functions, and has been implemented for rectangular thin plates only.

Chen and New [1999] used the DQ technique to discretize the derivatives of variable functions existing in the integral statements for variational methods, the Galerkin method, and so on, in deriving the finite element formulation, the discretizations of the static 3-D linear elasticity problem and the buckling problem of a plate by using the principle of minimum potential energy were illustrated. This method is named as the differential quadrature finite element method (DQFEM). Later, Haghghi *et al.* [2008] developed the coupled DQ-FE methods for two dimensional transient heat transfer analysis of functionally graded material. Nevertheless, shape functions are needed in both methods.

Zhong and Yu [2009] presented the weak form QEM for static plane elasticity problems by discretizing the energy functional using the DQ rules and the Gauss-Lobatto integral rules, whereas each sub-domain in the discretization of solution domain was called a quadrature element. This weak form QEM differs fundamentally with that of [Striz *et al.*, 1995; Striz *et al.*, 1997], and the strong form QEM of [Striz *et al.*, 1994; Zhong and He, 1998]. The weak form QEM is similar with the Ritz-Rayleigh method as well as the p -version while it exhibits distinct features of high order approximation and flexible geometric modeling capability.

Xing and Liu [2009] presented a differential quadrature finite element method (DQFEM) which was motivated by the complexity of imposing boundary conditions in DQM and the unsymmetrical element matrices in DQEM, the name is the same as that of [Chen and New, 1999], but the starting points and implementations are different. Compared with [Zhong and Yu, 2009] and [Chen and New, 1999], DQFEM [Xing and Liu, 2009] has the following novelties: (1) DQ rules are reformulated, and in conjunction with the Gauss-Lobatto integral rule are used to discretize the energy functional to derive the finite element formulation of thin plate for both regular and irregular domains. (2) The Lagrange interpolation functions are used as trial functions for C^1 problems, and the C^1 continuity requirements are accomplished through modifying the nodal parameters using DQ rules, the nodal

shapes functions as in standard FEM are not necessary. (3) The DQFE element matrices are symmetric, well conditioned, and computed efficiently by simple algebraic operations of the known weighting coefficient matrices of the reformulated DQ rules and Gauss-Lobatto integral rule.

In this paper, the differential quadrature finite element method is studied systematically, and the following novel works are included: DQFEM is viewed as a general method of formulating finite elements from lower order to higher order, the difficulty of formulating higher order finite elements are alleviated, especially for C^1 high order elements; the 1-D to 3-D DQFE stiffness and mass matrices and load vectors for C^0 and C^1 problems are given explicitly, which are significant to static and dynamic applications; it is shown that all C^0 DQFE mass matrices are diagonal, but they are obtained by using non-orthogonal polynomials and different from the conventional diagonal lumped mass matrices; the reformulated DQ rules for curvilinear quadrilateral domain and its implementation are also presented to improve its application; furthermore, the free vibration analyses of 2-D and 3-D plates with continuous and discontinuous boundaries and bending analyses of thin and Mindlin plates with arbitrary shapes are carried out.

The outline of this paper is as follows. The reformulation of DQM and its implementation are presented in Sec. 2. In Sec. 3, the DQFE stiffness and mass matrices and load vectors are given explicitly for rod, beam, plate, 2-D and 3-D elasticity problems, and the cubic Euler beam element matrices of DQFEM are compared with that of FEM. In Sec. 4, the numerical results are compared with some available results. Finally the conclusions are outlined.

2. The Reformulated Differential Quadrature Rule

The survey paper [Bert and Malik, 1996] has presented the details of DQM, only the reformulated DQ rules for curvilinear quadrilateral domain and its implementations are given below. DQM has been applied to irregular domains with the help of the natural-to-Cartesian geometric mapping using the serendipity-family interpolation functions [Bert and Malik, 1996; Xing and Liu, 2009] or the blending functions which permit exact mapping [Malik and Bert, 2000].

The mapping using serendipity-family interpolation functions is applicable to arbitrary domain. For an arbitrary quadrilateral domain as shown in Fig. 1, the geometric mapping has the form

$$\begin{cases} x(\xi, \eta) = \sum S_k(\xi, \eta)x_k \\ y(\xi, \eta) = \sum S_k(\xi, \eta)y_k \end{cases} \quad -1 \leq \xi, \eta \leq 1 \quad (1)$$

where x_k, y_k ; ($k = 1, 2, \dots, N_s$) are the coordinates of N_s boundary grid points in the Cartesian x - y plane, $S_k(\xi, \eta)$ the serendipity interpolations defined in the natural ξ - η plane. Since the base function S_k has a unity value at the k th node and zeros at the remaining ($N_s - 1$) nodes, the domain mapped by Eq. (1) and the given quadrilateral domain matches exactly at least at the nodal points.

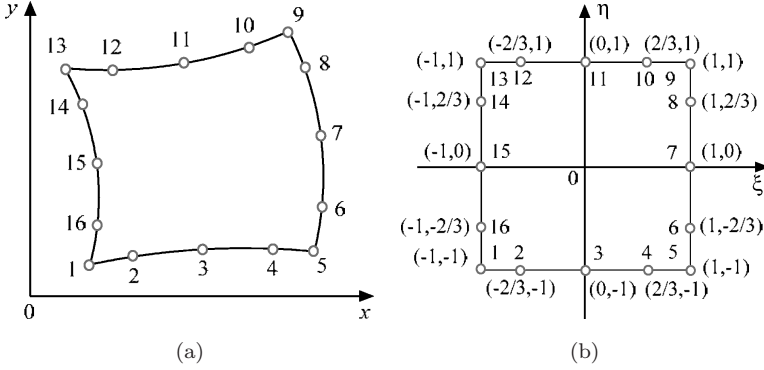


Fig. 1. (a) A curvilinear quadrilateral region in Cartesian x - y plane; (b) a square parent domain in natural ξ - η plane.

Subsequently, we should express the derivatives of a function $f(x, y)$ with respect to x, y coordinates in terms of its derivatives in ξ - η coordinates. Using the chain rule of differentiation results in

$$\frac{\partial f}{\partial x} = \frac{1}{|\mathbf{J}|} \left(\frac{\partial y}{\partial \eta} \frac{\partial f}{\partial \xi} - \frac{\partial y}{\partial \xi} \frac{\partial f}{\partial \eta} \right), \quad \frac{\partial f}{\partial y} = \frac{1}{|\mathbf{J}|} \left(\frac{\partial x}{\partial \xi} \frac{\partial f}{\partial \eta} - \frac{\partial x}{\partial \eta} \frac{\partial f}{\partial \xi} \right) \quad (2)$$

where the determinant $|\mathbf{J}|$ of the Jacobian $\mathbf{J} = \partial(x, y)/\partial(\xi, \eta)$ is

$$|\mathbf{J}| = \frac{\partial x}{\partial \xi} \frac{\partial y}{\partial \eta} - \frac{\partial y}{\partial \xi} \frac{\partial x}{\partial \eta} \quad (3)$$

Then the partial derivatives $\partial f/\partial x$ and $\partial f/\partial y$ at grid point $x_{ij} = x(\xi_i, \eta_j), y_{ij} = y(\xi_i, \eta_j)$ in the mapped curvilinear quadrilateral domain can be computed using DQ rules, as

$$\left(\frac{\partial f}{\partial x} \right)_{ij} = \frac{1}{|\mathbf{J}|_{ij}} \left[\left(\frac{\partial y}{\partial \eta} \right)_{ij} \left(\sum_{m=1}^M A_{im}^{(1)} f_{mj} \right) - \left(\frac{\partial y}{\partial \xi} \right)_{ij} \left(\sum_{n=1}^N B_{jn}^{(1)} f_{in} \right) \right] \quad (4)$$

$$\left(\frac{\partial f}{\partial y} \right)_{ij} = \frac{1}{|\mathbf{J}|_{ij}} \left[\left(\frac{\partial x}{\partial \xi} \right)_{ij} \left(\sum_{n=1}^N B_{jn}^{(1)} f_{in} \right) - \left(\frac{\partial x}{\partial \eta} \right)_{ij} \left(\sum_{m=1}^M A_{im}^{(1)} f_{mj} \right) \right] \quad (5)$$

where M and N are the numbers of grid points in x (or ξ)-direction and y -(or η) direction, respectively. $A_{ij}^{(r)}$ and $B_{ij}^{(s)}$ are the weighting coefficients associated with the r th-order and s th-order partial derivative of f with respect to ξ and η at the discrete point ξ_i and η_j , respectively. Equations (4) and (5) define the DQ rules of the first order partial derivatives with respect to the Cartesian x, y coordinates for irregular domain. Certainly, these rules can also be written in a compact form using

a single index notation for grid points, as

$$\left. \frac{\partial f}{\partial x} \right|_k = \sum_{m=1}^{M \times N} \bar{A}_{km}^{(1)} \bar{f}_m, \quad \left. \frac{\partial f}{\partial y} \right|_k = \sum_{m=1}^{M \times N} \bar{B}_{km}^{(1)} \bar{f}_m \quad (6)$$

where $k = (j - 1)M + i$, $\bar{A}_{km}^{(1)}$ and $\bar{B}_{km}^{(1)}$ are respectively the assemblages of $A_{ij}^{(1)}$ and $B_{ij}^{(1)}$ according to \bar{f}_m defined as follows

$$\bar{f}_m = f_{ij} = f(\xi_i, \eta_j), \quad m = (j - 1)M + i \quad (7)$$

where $i = 1, \dots, M; j = 1, \dots, N$, and the elements of $\bar{\mathbf{A}}^{(1)}$ and $\bar{\mathbf{B}}^{(1)}$ can be computed from $\mathbf{A}^{(1)}$ and $\mathbf{B}^{(1)}$ for each (i, j) by

$$\begin{aligned} \mathbf{a}((j - 1) \times M + m) &= \mathbf{A}^{(1)}(i, m), \quad m = 1, \dots, M \\ \mathbf{b}((n - 1) \times M + i) &= \mathbf{B}^{(1)}(j, n), \quad n = 1, \dots, N \end{aligned} \quad (8)$$

$$\begin{aligned} \bar{\mathbf{A}}^{(1)}(k, :) &= \frac{1}{|\mathbf{J}|_{ij}} \left[\left(\frac{\partial y}{\partial \eta} \right)_{ij} \mathbf{a} - \left(\frac{\partial y}{\partial \xi} \right)_{ij} \mathbf{b} \right] \\ \bar{\mathbf{B}}^{(1)}(k, :) &= \frac{1}{|\mathbf{J}|_{ij}} \left[\left(\frac{\partial x}{\partial \xi} \right)_{ij} \mathbf{b} - \left(\frac{\partial x}{\partial \eta} \right)_{ij} \mathbf{a} \right] \end{aligned} \quad (9)$$

The high order DQ rules in the mapped region can be written similarly as

$$\left. \frac{\partial^r f}{\partial x^r} \right|_k = \sum_{m=1}^{M \times N} \bar{A}_{km}^{(r)} \bar{f}_m, \quad \left. \frac{\partial^s f}{\partial y^s} \right|_k = \sum_{m=1}^{M \times N} \bar{B}_{km}^{(s)} \bar{f}_m, \quad \left. \frac{\partial^{r+s} f}{\partial x^r \partial y^s} \right|_k = \sum_{m=1}^{M \times N} \bar{F}_{km}^{(r+s)} \bar{f}_m \quad (10)$$

where the weighting coefficients can be obtained using the recurrence relationships

$$\begin{aligned} \bar{\mathbf{A}}^{(r)} &= \bar{\mathbf{A}}^{(1)} \bar{\mathbf{A}}^{(r-1)}, \quad \bar{\mathbf{B}}^{(s)} = \bar{\mathbf{B}}^{(1)} \bar{\mathbf{B}}^{(s-1)} \quad (r, s \geq 2), \\ \bar{\mathbf{F}}^{(r+s)} &= \bar{\mathbf{A}}^{(r)} \bar{\mathbf{B}}^{(s)} \quad (r, s \geq 1). \end{aligned} \quad (11)$$

The DQ approximations for the first-order derivatives of function $f(x, y, z)$ defined over a regular hexahedron are required for the 3-D formulation in present paper, and can be written as

$$\left. \frac{\partial f}{\partial x} \right|_{ijk} = \sum_{m=1}^M A_{im}^{(1)} f_{mjk}, \quad \left. \frac{\partial f}{\partial y} \right|_{ijk} = \sum_{n=1}^N B_{jn}^{(1)} f_{ink}, \quad \left. \frac{\partial f}{\partial z} \right|_{ijk} = \sum_{l=1}^L C_{kl}^{(1)} f_{ijl} \quad (12)$$

where $A_{ij}^{(1)}$, $B_{ij}^{(1)}$ and $C_{ij}^{(1)}$ are the weighting coefficients associated with the first-order partial derivative of $f(x, y, z)$ with respect to x , y , and z at the discrete point x_i , y_i , and z_i , respectively.

For 3-D irregular hexahedron, using the corresponding isoparametric mapping and in the same way as in Eqs. (2)–(10), the first-order derivatives of function $f(x, y, z)$ in the mapped region can be written as

$$\left. \frac{\partial f}{\partial x} \right|_q = \sum_{p=1}^{M \times N \times L} \bar{A}_{qp}^{(1)} \bar{f}_p, \quad \left. \frac{\partial f}{\partial y} \right|_q = \sum_{p=1}^{M \times N \times L} \bar{B}_{qp}^{(1)} \bar{f}_p, \quad \left. \frac{\partial f}{\partial z} \right|_q = \sum_{p=1}^{M \times N \times L} \bar{C}_{qp}^{(1)} \bar{f}_p \quad (13)$$

where

$$\bar{f}_p = f_{ijk} = f(\xi_i, \eta_j, \zeta_k), \quad \text{for } i = 1, 2, \dots, M; \quad j = 1, 2, \dots, N; \quad k = 1, 2, \dots, L. \quad (14)$$

$$p, q = (k - 1) \times L \times N + (j - 1) \times N + i. \quad (15)$$

The weighting coefficients of Eq. (13) can be obtained through assembling those of Eq. (12) according to the similar method for 2-D case as above.

3. The Differential Quadrature Finite Element Method

The differential quadrature finite element method was developed in reference [Xing and Liu, 2009] where the DQ and Gauss-Lobatto quadrature rules were used to discretize the energy functional, by which the free vibrations of thin plates were investigated extensively.

Here we extend the DQFEM to rod, beam, thick plate, plane and three dimensional problems. For linear elastic bodies, the total potential energy Π involves the strain energy and work potential, and is given by

$$\Pi = \frac{1}{2} \iiint_V \boldsymbol{\varepsilon}^T \mathbf{D} \boldsymbol{\varepsilon} dV - \iint_S \mathbf{u}^T \mathbf{q} dS \quad (16)$$

where $\boldsymbol{\varepsilon}$ and \mathbf{D} are the strain field vector and the material matrix, respectively, \mathbf{u} is the displacement field vector, and \mathbf{q} the distributed surface force vector. The kinetic energy functional is given by

$$T = \frac{1}{2} \iiint_V \rho \dot{\mathbf{u}}^T \dot{\mathbf{u}} dV \quad (17)$$

where $\dot{\mathbf{u}}$ is the velocity field vector, ρ the volume density. Then the element matrices of different kinds of structures can be obtained from the discrete quadratic forms of Π and T .

3.1. Rod element

Consider a uniform rod element of length l , cross section area S . Assuming that the longitudinal displacement function is

$$u(x) = \sum_{i=1}^M l_i(x) u_i \quad (18)$$

where l_i are the Lagrange polynomials, $u_i = u(x_i)$ the displacements of the Gauss Lobatto quadrature points or the nodal displacements of the DQ finite rod element, x_j the Gauss-Lobatto node coordinates, M the total node number. Using DQ and Gauss-Lobatto quadrature rules, Eqs. (16) and (17) can be written as

$$\Pi = \frac{1}{2} \int_0^l ES \left(\frac{\partial u}{\partial x} \right)^2 dx - \int_0^l q u dx = \frac{1}{2} \mathbf{u}^T \mathbf{A}^{(1)T} E S \mathbf{C} \mathbf{A}^{(1)} \mathbf{u} - \mathbf{u}^T (\mathbf{C} \mathbf{q}) \quad (19)$$

$$T = \frac{1}{2} \int_0^l \rho S \dot{u}^2 dx = \frac{1}{2} \dot{\mathbf{u}}^T (\rho S \mathbf{C}) \dot{\mathbf{u}} \quad (20)$$

where E is the Young's modulus, $\mathbf{u}^T = [u_1 \quad u_2 \quad \cdots \quad u_M]$ the nodal displacement vector, $\mathbf{q}^T = [q(x_1) \quad q(x_2) \quad \cdots \quad q(x_M)]$ the nodal load vector, $\mathbf{A}^{(1)T} = (\mathbf{A}^{(1)})^T$ where $\mathbf{A}^{(1)}$ indicates the weighting coefficient matrix of DQ rules for the first-order derivatives [Bert and Malik, 1996; Xing and Liu, 2009] with respect to the Gauss-Lobatto nodes, and

$$\mathbf{C} = \text{diag}(C_1 \quad C_2 \quad \cdots \quad C_M) \quad (21)$$

where C_j are the weighting coefficients of Gauss-Lobatto integration. Therefore, the stiffness matrix \mathbf{K} , mass matrix \mathbf{M} and load vector \mathbf{R} are

$$\mathbf{K} = E S \mathbf{A}^{(1)T} \mathbf{C} \mathbf{A}^{(1)}, \quad \mathbf{M} = \rho S \mathbf{C}, \quad \mathbf{R} = \mathbf{C} \mathbf{q} \quad (22)$$

It is noticeable that the finite element matrices in DQFEM can be obtained by simple algebraic operations of the weighting coefficient matrices of DQ rule and Gauss-Lobatto integral rule, and that the mass matrix \mathbf{M} of rod element is diagonal. For the 3-degree-of-freedom element where the nodes of DQFEM and FEM are the same, the element stiffness matrices and load vectors of both methods must be identical, but the mass element matrices are different, hence only the element mass matrix of DQFEM is given below, as

$$\mathbf{M} = \frac{\rho S l}{6} \begin{bmatrix} 1 & 0 & 0 \\ 0 & 4 & 0 \\ 0 & 0 & 1 \end{bmatrix} \quad (23)$$

It is noteworthy that the diagonal element ratios of mass matrices of both methods are the same. Although the mass matrix in Eq. (22) is diagonal, it is not the same as the lumped mass matrix of FEM.

3.2. Euler beam element

Consider a uniform Euler beam element with length l and cross section area S . Assuming that the deflection function is

$$w(x) = \sum_{i=1}^M l_i(x)w_i \tag{24}$$

where $w_i = w(x_i)$ are the deflections of the Gauss Lobatto quadrature nodes of the DQ finite beam element. Similarly as in Sec. 3.1, using DQ and Gauss-Lobatto quadrature rules, Eqs. (16) and (17) can be written as

$$\begin{aligned} \Pi &= \frac{1}{2} \int_0^l EI \left(\frac{\partial^2 w}{\partial x^2} \right) dx - \int_0^l q w dx = \frac{1}{2} \bar{\mathbf{w}}^T \mathbf{A}^{(2)T} \mathbf{EICA}^{(2)} \bar{\mathbf{w}} - \bar{\mathbf{w}}^T \mathbf{C} \mathbf{q} \\ T &= \frac{1}{2} \int_0^l \rho S \dot{w}^2 dx = \frac{1}{2} \dot{\bar{\mathbf{w}}}^T (\rho S \mathbf{C}) \dot{\bar{\mathbf{w}}} \end{aligned} \tag{25}$$

where I is the moment of inertia, and

$$\bar{\mathbf{w}}^T = [w_1 \quad w_2 \quad \cdots \quad w_M] \tag{26}$$

In order to construct element satisfying C^1 inter-element continuity requirements, the element displacement vector should be

$$\mathbf{w}^T = [w_1 \quad w'_1 \quad w_3 \quad \cdots \quad w_{M-2} \quad w_M \quad w'_M] \tag{27}$$

Using DQ rules one can find the relation between \mathbf{w} and $\bar{\mathbf{w}}$ as

$$\mathbf{w} = \mathbf{Q} \bar{\mathbf{w}} \tag{28}$$

where

$$\mathbf{Q} = \begin{bmatrix} 1 & 0 & 0 & \cdots & 0 & 0 \\ A_{1,1}^{(1)} & A_{1,2}^{(1)} & A_{1,3}^{(1)} & \cdots & A_{1,M-1}^{(1)} & A_{1,M}^{(1)} \\ 0 & 0 & 1 & \cdots & 0 & 0 \\ \vdots & \vdots & \vdots & \ddots & \vdots & \vdots \\ 0 & 0 & 0 & \cdots & 0 & 1 \\ A_{M,1}^{(1)} & A_{M,2}^{(1)} & A_{M,3}^{(1)} & \cdots & A_{M,M-1}^{(1)} & A_{M,M}^{(1)} \end{bmatrix} \tag{29}$$

Substituting Eq. (28) into Eq. (25), the stiffness matrix, mass matrix and load vector of the DQ finite Euler beam element are obtained as

$$\mathbf{K} = \mathbf{EI} \mathbf{Q}^{-T} \mathbf{A}^{(2)T} \mathbf{C} \mathbf{A}^{(2)} \mathbf{Q}^{-1}, \quad \mathbf{M} = \mathbf{Q}^{-T} (\rho S \mathbf{C}) \mathbf{Q}^{-1}, \quad \mathbf{R} = \mathbf{Q}^{-T} \mathbf{C} \mathbf{q} \tag{30}$$

It is readily shown that the transformation matrix \mathbf{Q} in Eq. (29) is well conditioned in general. In the same way as in Eq. (30), the construction of element with C^n continuity is possible. Similarly as in rod case discussed above, for a beam subjected to uniformly distributed load q_0 , the element stiffness matrices and load vectors of FEM and DQFEM are the same, but the Lagrange polynomials are used in Eq. (24)

while the Hermite interpolation functions are used in FEM. The 4-degree-of-freedom element mass matrix in DQFEM is

$$M = \frac{\rho Sl}{420} \begin{bmatrix} 156.8 & 22.4l & 53.2 & -12.6l \\ 22.4l & 4.2l^2 & 12.6l & -2.8l^2 \\ 53.2 & 12.6l & 156.8 & -22.4l \\ -12.6l & -2.8l^2 & -22.4l & 4.2l^2 \end{bmatrix} \quad (31)$$

Apparently, the mass matrix of DQFEM has small difference from that of FEM.

3.3. Plane element

Consider a curvilinear quadrilateral domain with uniform thickness h , as shown in Fig. 1, the displacement fields have the forms

$$[u(x, y), v(x, y)] = \sum_{i=1}^M \sum_{j=1}^N l_i(x)l_j(y)[u_{ij}, v_{ij}] \quad (32)$$

The strain-displacement relations of plane problems are

$$\begin{bmatrix} \varepsilon_x \\ \varepsilon_y \\ \gamma_{xy} \end{bmatrix} = \begin{bmatrix} \partial/\partial x & 0 \\ 0 & \partial/\partial y \\ \partial/\partial y & \partial/\partial x \end{bmatrix} \begin{bmatrix} u \\ v \end{bmatrix} \quad (33)$$

Define the following element displacement vectors

$$\mathbf{u}^T = [u_{11} \ \cdots \ u_{M1} \ u_{12} \ \cdots \ u_{M2} \ \cdots \ u_{1N} \ \cdots \ u_{MN}] \quad (34a)$$

$$\mathbf{v}^T = [v_{11} \ \cdots \ v_{M1} \ v_{12} \ \cdots \ v_{M2} \ \cdots \ v_{1N} \ \cdots \ v_{MN}] \quad (34b)$$

then by inserting Eq. (32) into Eq. (33), one can obtain the corresponding nodal strain vector

$$\begin{bmatrix} \varepsilon_x \\ \varepsilon_y \\ \gamma_{xy} \end{bmatrix} = \begin{bmatrix} \bar{\mathbf{A}}^{(1)} & \mathbf{0} \\ \mathbf{0} & \bar{\mathbf{B}}^{(1)} \\ \bar{\mathbf{B}}^{(1)} & \bar{\mathbf{A}}^{(1)} \end{bmatrix} \begin{bmatrix} u \\ v \end{bmatrix} \quad (35)$$

where the DQ rule and Gauss-Lobatto rule have been involved, $\bar{\mathbf{A}}^{(1)}$, $\bar{\mathbf{B}}^{(1)}$ are given in Eq. (9), and the three nodal strain vectors have the same form as in Eq. (34). Thus, we can obtain the matrices of the DQ finite curvilinear quadrilateral plane element, for plane stress problem, they are

$$\mathbf{K} = c \begin{bmatrix} \bar{\mathbf{A}}^{(1)T} \mathbf{C} \bar{\mathbf{A}}^{(1)} + v_1 \bar{\mathbf{B}}^{(1)T} \mathbf{C} \bar{\mathbf{B}}^{(1)} & v \bar{\mathbf{A}}^{(1)T} \mathbf{C} \bar{\mathbf{B}}^{(1)} + v_1 \bar{\mathbf{B}}^{(1)T} \mathbf{C} \bar{\mathbf{A}}^{(1)} \\ v \bar{\mathbf{B}}^{(1)T} \mathbf{C} \bar{\mathbf{A}}^{(1)} + v_1 \bar{\mathbf{A}}^{(1)T} \mathbf{C} \bar{\mathbf{B}}^{(1)} & \bar{\mathbf{B}}^{(1)T} \mathbf{C} \bar{\mathbf{B}}^{(1)} + v_1 \bar{\mathbf{A}}^{(1)T} \mathbf{C} \bar{\mathbf{A}}^{(1)} \end{bmatrix} \quad (36)$$

$$\mathbf{M} = \rho h \begin{bmatrix} \mathbf{C} & \mathbf{0} \\ \mathbf{0} & \mathbf{C} \end{bmatrix}, \quad \mathbf{R} = \begin{bmatrix} \mathbf{C} \mathbf{q}_u \\ \mathbf{C} \mathbf{q}_v \end{bmatrix} \quad (37)$$

where the corresponding nodal displacement vector is $[\mathbf{u}^T \ \mathbf{v}^T]$, $c = Eh/(1 - \nu^2)$, $v_1 = (1 - \nu)/2$, $\mathbf{C} = \text{diag}(\mathbf{J}_k \mathbf{C}_k)$, $\mathbf{J}_k = |\mathbf{J}|_{ij}$ is the determinant of the Jacobian \mathbf{J} ,

$C_k = C_i^\xi C_j^\eta$, $k = (j-1)M + i$; C_i^ξ and C_j^η the Gauss-Lobatto weights with respect to ξ and η , respectively; \mathbf{q}_u and \mathbf{q}_v are the nodal load vectors whose elements are the nodal function values of the distributed force and arranged similarly as in Eq. (34). To replace E and ν in Eq. (36) with $E/(1-\nu^2)$ and $\nu/(1-\nu)$ will yield the stiffness matrix of plane strain element.

3.4. Kirchhoff plate element

The thin curvilinear quadrilateral plate element of DQFEM, as shown in Fig. 2, has been well established [Xing and Liu, 2009], for completeness of present paper, the main results are given below. The deflection function is defined in terms of Lagrange polynomials as follows

$$w(x, y) = \sum_{i=1}^M \sum_{j=1}^N l_i(x)l_j(y)w_{ij} \tag{38}$$

In order to satisfy the C^1 inter-element compatibility conditions, the displacement vector is assumed to be

$$\mathbf{w} = [w_m, w_{mx}, w_{my}, w_{mxy} (i = 1, M; j = 1, N), w_m, w_{mx}, (i = 3, \dots, M - 2; j = 1, N), w_m, w_{my}, (i = 1, M; j = 3, \dots, N - 2), w_m, (i = 3, \dots, M - 2; j = 3, \dots, N - 2)] \tag{39}$$

where the scale $m = (j - 1)M + i$, $w_{mx} = (\partial w / \partial x)_m$, $w_{my} = (\partial w / \partial y)_m$, and $w_{mxy} = (\partial^2 w / \partial x \partial y)_m$. The element matrices are given by

$$\mathbf{K} = D\mathbf{Q}^{-T} [\bar{\mathbf{A}}^{(2)T} \mathbf{C} \bar{\mathbf{A}} + \bar{\mathbf{B}}^{(2)T} \mathbf{C} \bar{\mathbf{B}}^{(2)} + \nu (\bar{\mathbf{A}}^{(2)T} \mathbf{C} \bar{\mathbf{B}}^{(2)} + \bar{\mathbf{B}}^{(2)T} \mathbf{C} \bar{\mathbf{A}}^{(2)}) + 2(1 - \nu) \bar{\mathbf{F}}^{(2)T} \mathbf{C} \bar{\mathbf{F}}^{(2)}] \mathbf{Q}^{-1} \tag{40}$$

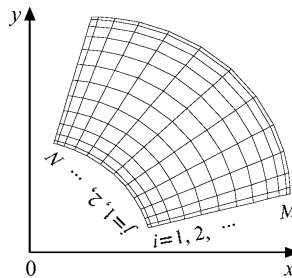


Fig. 2. A sectorial region.

$$\begin{aligned} \mathbf{M} &= \mathbf{Q}^{-T}(\rho h \mathbf{C})\mathbf{Q}^{-1} \\ \mathbf{R} &= \mathbf{Q}^{-T}(\mathbf{C}\mathbf{q}) \end{aligned} \tag{41}$$

where $\bar{\mathbf{A}}^{(2)}$, $\bar{\mathbf{B}}^{(2)}$ and $\bar{\mathbf{F}}^{(2)} = \bar{\mathbf{A}}^{(1)}\bar{\mathbf{B}}^{(1)}$ are the weighting coefficient matrices defined by Eq. (11), $D= Eh^3/12(1-v^2)$ is bending rigidity of plate, h is the thickness, \mathbf{C} is identical to that of in-plane case.

3.5. Mindlin plate element

In Mindlin plate theory, one can choose the deflection w and two rotations θ_x and θ_y of the normal line with respect to the middle surface as the generalized displacements which can be expressed as

$$[w, \theta_x, \theta_y] = \sum_{i=1}^M \sum_{j=1}^N l_i(x)l_j(y)[w_{ij}, \theta_{xij}, \theta_{yij}] \tag{42}$$

Define the nodal displacement vector as $[\boldsymbol{\theta}_x^T \ \boldsymbol{\theta}_y^T \ \mathbf{w}^T]$ whose elements are arranged as in Eq. (34), one can determine the DQ Mindlin plate element matrices as

$$\mathbf{K} = D \begin{bmatrix} \mathbf{K}_{11} & & \text{sym} \\ \mathbf{K}_{21} & \mathbf{K}_{22} & \\ \mathbf{K}_{31} & \mathbf{K}_{32} & \mathbf{K}_{33} \end{bmatrix}, \quad \mathbf{M} = \rho \begin{bmatrix} J\mathbf{C} & & \text{sym} \\ \mathbf{0} & J\mathbf{C} & \\ \mathbf{0} & \mathbf{0} & h\mathbf{C} \end{bmatrix}, \quad \mathbf{R} = \begin{bmatrix} \mathbf{C}\mathbf{m}_x \\ \mathbf{C}\mathbf{m}_y \\ \mathbf{C}\mathbf{q}_w \end{bmatrix} \tag{43a}$$

$$\begin{bmatrix} \mathbf{K}_{11} \\ \mathbf{K}_{22} \\ \mathbf{K}_{33} \end{bmatrix} = \begin{bmatrix} 1 & v_1 & v_s \\ v_1 & 1 & v_s \\ v_s & v_s & 0 \end{bmatrix} \begin{bmatrix} \bar{\mathbf{A}}^{(1)T} \mathbf{C} \bar{\mathbf{A}}^{(1)} \\ \bar{\mathbf{B}}^{(1)T} \mathbf{C} \bar{\mathbf{B}}^{(1)} \\ \mathbf{C} \end{bmatrix}, \quad \begin{aligned} \mathbf{K}_{21} &= v\bar{\mathbf{B}}^{(1)T} \mathbf{C} \bar{\mathbf{A}}^{(1)} + v_1\bar{\mathbf{A}}^{(1)T} \mathbf{C} \bar{\mathbf{B}}^{(1)} \\ \mathbf{K}_{31} &= -v_s\bar{\mathbf{A}}^{(1)T} \mathbf{C} \\ \mathbf{K}_{32} &= -v_s\bar{\mathbf{B}}^{(1)T} \mathbf{C} \end{aligned} \tag{43b}$$

where $v_1 = (1-v)/2$, $v_s = 6\kappa(1-v)/h^2$, $J = h^3/12$; \mathbf{m}_x and \mathbf{m}_y are the nodal bending moment vectors with respect to x and y directions, \mathbf{q}_w is the nodal force vector with respect to z direction, they have the same form as that of Eq. (34). \mathbf{C} is identical to that of in-plane case, the shear rigidity of Mindlin plate is $\kappa Gh = v_s D$ where κ is the shear correction factor, G the shear modulus.

3.6. Three dimensional element

For 3-D problems, the translational displacements in DQFEM are given by

$$[u, v, w] = \sum_{i=1}^M \sum_{j=1}^N \sum_{k=1}^L l_i(x)l_j(y)l_k(z)[u_{ijk}, v_{ijk}, w_{ijk}] \tag{44}$$

Define the nodal displacement vector as $[\mathbf{u}^T \ \mathbf{v}^T \ \mathbf{w}^T]$ whose elements are arranged as in Eqs. (14) and (15), in the same way as in-plane and Mindlin plate cases, one can

determine the 3-D element matrices of DQFEM as

$$K = \frac{G}{\nu_2} \begin{bmatrix} K_{11} & & \text{sym} \\ K_{21} & K_{22} & \\ K_{31} & K_{32} & K_{33} \end{bmatrix}, \quad M = \rho \begin{bmatrix} C & & \text{sym} \\ \mathbf{0} & C & \\ \mathbf{0} & \mathbf{0} & C \end{bmatrix}, \quad R = \begin{bmatrix} Cq_u \\ Cq_v \\ Cq_w \end{bmatrix} \quad (45a)$$

$$\begin{bmatrix} K_{11} \\ K_{22} \\ K_{33} \end{bmatrix} = \begin{bmatrix} v_1 & v_2 & v_2 \\ v_2 & v_1 & v_2 \\ v_2 & v_2 & v_1 \end{bmatrix} \begin{bmatrix} \bar{A}^{(1)T} C \bar{A}^{(1)} \\ \bar{B}^{(1)T} C \bar{B}^{(1)} \\ \bar{C}^{(1)T} C \bar{C}^{(1)} \end{bmatrix}, \quad \begin{aligned} K_{21} &= v \bar{B}^{(1)T} C \bar{A}^{(1)} + v_2 \bar{A}^{(1)T} C \bar{B}^{(1)} \\ K_{31} &= v \bar{C}^{(1)T} C \bar{A}^{(1)} + v_2 \bar{A}^{(1)T} C \bar{C}^{(1)} \\ K_{32} &= v \bar{C}^{(1)T} C \bar{B}^{(1)} + v_2 \bar{B}^{(1)T} C \bar{C}^{(1)} \end{aligned} \quad (45b)$$

where $\bar{A}^{(1)}$, $\bar{B}^{(1)}$ and $\bar{C}^{(1)}$ are the weighting coefficient matrices whose element are used in Eq. (13), $v_1 = 1 - v$, $v_2 = 0.5 - v$, $C = \text{diag}(J_p C_p)$ where $J_p = |J|_{ijk}$ is the determinant of the Jacobian J of 3-D isoparametric transformation, $C_p = C_i^\xi C_j^\eta C_k^\zeta$, the scale p is calculated from Eq. (15), C_i^ξ , C_j^η and C_k^ζ are the Gauss-Lobatto weights with respect to ξ , η and ζ , respectively.

4. Numerical Comparisons

The results presented in this section aims at demonstrating the high accuracy and rapid convergence of the DQFEM. This is done through 2-D and 3-D free vibration analyses of plates (Tables 1–3) and static plate bending analyses (Table 4), the free vibration analyses of rectangular plates with discontinuous boundaries (Table 5).

For free vibration analyses, the frequencies are given in dimensionless form denoted by Ω which is included in the tables where the results for various boundary conditions are given for a range of the sampling points to show clearly the convergence behavior of the solution method. In all cases, Poisson’s ratio is 0.3.

In Table 1, comparison and convergence studies are carried out for in-plane free vibration of six types of rectangular plate, i.e., two completely free plates, two clamped plates, two simply supported plates, with aspect ratio $a/b = 1$ and 2, respectively. The DQFEM solutions are compared with the Rayleigh-Ritz solutions [Bardell *et al.*, 1996]. For the rectangular plates with aspect ratio $a/b = 1$, the results of the completely free, simply supported, and clamped plates converge when grid size equals 7×7 , 8×8 , and 9×9 , respectively. Thus, one can say that completely free plate converges fastest, while clamped plate converges slowest. It can be seen that all of the frequencies of DQFEM are exactly the same as those of Rayleigh-Ritz method.

Table 2 presents comparison studies of flexural free vibration of six triangular thin plates (see Fig. 3) with three combinations of simply supported, clamped and free edges, namely CCC, SSS and SCF. SCF implies the side (1), side (2) and side (3) of a triangle are simply supported, clamped and free, respectively. The triangular plates are divided into three sub quadrilateral elements in calculation. It can be seen that DQFEM is capable of producing accurate results when the grid size of each

subelement is 10×10 . The DQFEM solutions agree with the Rayleigh-Ritz solutions [Karunasena and Kitipornchai, 1997], at least to three significant digits, and with the superposition solutions [Gorman, 1983; Gorman, 1986; Gorman, 1989], to two or three significant digits.

In Table 3, a comparison study has been given for 3-D free vibration of circular plates with clamped and free boundary conditions. The DQFEM solutions are given for two free circular plates with relative thickness $h/R = 0.1$ and 0.2 , and a clamped plate with relative thickness $h/R = 0.01$. Convergent DQFEM solutions are obtained when the grid size equals $13 \times 13 \times 6$ and $15 \times 15 \times 5$ for free and

Table 1. Convergence validation of the natural frequencies $\Omega = \omega a \sqrt{\rho(1 - \mu^2)/E}$ for in-plane free vibrations of isotropic rectangular plates.

a/b	Grid points $M \times N$	Mode sequence number					
		1	2	3	4	5	6
Completely free plates							
1.0	5×5	2.332	2.464	2.464	2.630	2.991	3.457
	6×6	2.321	2.473	2.473	2.628	2.988	3.453
	7×7	2.321	2.472	2.472	2.628	2.987	3.452
	8×8	2.321	2.472	2.472	2.628	2.987	3.452
	Ref. a	2.321	2.472	2.472	2.628	2.987	3.452
2.0	8×5	1.954	2.961	3.267	4.731	4.795	5.201
	9×6	1.954	2.961	3.267	4.728	4.784	5.206
	10×7	1.954	2.961	3.267	4.726	4.784	5.205
	11×8	1.954	2.961	3.267	4.726	4.784	5.205
	Ref. a	1.954	2.961	3.267	4.726	4.784	5.205
Clamped plates							
1.0	7×7	3.555	3.555	4.236	5.191	5.863	5.863
	8×8	3.555	3.555	4.235	5.186	5.859	5.901
	9×9	3.555	3.555	4.235	5.186	5.859	5.894
	10×10	3.555	3.555	4.235	5.186	5.859	5.895
	Ref. a	3.555	3.555	4.235	5.186	5.859	5.895
2.0	9×6	4.789	6.379	6.711	7.049	7.609	8.116
	10×7	4.789	6.379	6.712	7.049	7.609	8.142
	11×8	4.789	6.379	6.712	7.049	7.608	8.140
	12×9	4.789	6.379	6.712	7.049	7.608	8.140
	Ref. a	4.789	6.379	6.712	7.049	7.608	8.140
Simply supported plates							
1.0	6×6	1.859	1.859	2.628	3.699	3.699	4.157
	7×7	1.859	1.859	2.628	3.718	3.718	4.157
	8×8	1.859	1.859	2.628	3.717	3.717	4.156
	9×9	1.859	1.859	2.628	3.717	3.717	4.156
	Ref. a	1.859	1.859	2.628	3.717	3.717	4.156
2.0	8×5	1.859	3.716	3.717	4.156	5.258	5.587
	9×6	1.859	3.717	3.717	4.156	5.257	5.574
	10×7	1.859	3.717	3.717	4.156	5.257	5.576
	11×8	1.859	3.717	3.717	4.156	5.257	5.576
	Ref. a	1.859	3.717	3.717	4.156	5.257	5.576

Ref. a: [Bardell *et al.*, 1996].

Table 2. The first four flexural free vibration frequencies $\Omega = \omega(a^2/\pi^2)\sqrt{\rho h/D}$ of triangular thin plates.

$M_\xi = N_\eta$	Mode sequences							
	1	2	3	4	1	2	3	4
	CCC Plate ($b/a = 1$)				CCC Plate ($b/a = 2$)			
	The Rayleigh-Ritz method based on Mindlin plate theory ($h/a = 0.001$) [Karunasena and Kitipornchai, 1997]							
	9.503	15.988	19.741	24.655	5.415	8.355	11.518	12.357
	The superposition method [Gorman, 1986]							
	9.510	15.978	19.737	24.601	5.416	8.351	11.500	12.351
	The differential quadrature finite element method							
10	9.489	15.978	19.751	24.589	5.407	8.332	11.519	12.347
12	9.496	15.984	19.742	24.595	5.411	8.342	11.508	12.346
14	9.500	15.986	19.738	24.598	5.413	8.347	11.504	12.346
16	9.501	15.987	19.736	24.600	5.414	8.349	11.501	12.345
18	9.502	15.987	19.735	24.600	5.414	8.350	11.500	12.345
20	9.502	15.987	19.735	24.600	5.415	8.351	11.500	12.345
	SSS Plate ($b/a=1$)				SSS Plate ($b/a = 2$)			
	The Rayleigh-Ritz method based on Mindlin plate theory ($h/a = 0.001$) [Karunasena and Kitipornchai, 1997]							
	5.000	9.999	13.000	17.005	2.813	5.054	7.569	8.241
	The superposition method [Gorman, 1983]							
	5.000	10.000	13.000	17.002	2.813	5.054	7.566	8.239
	DQFEM based on thin plate theory							
10	4.988	9.999	12.999	16.975	2.806	5.047	7.560	8.237
12	4.994	10.000	13.000	16.988	2.809	5.051	7.563	8.238
14	4.997	10.000	13.000	16.994	2.811	5.052	7.565	8.239
16	4.998	10.000	13.000	16.996	2.812	5.053	7.565	8.239
18	4.999	10.000	13.000	16.998	2.812	5.054	7.565	8.239
20	4.999	10.000	13.000	16.999	2.812	5.054	7.566	8.239
	SCF Plate ($b/a = 0.5$)				SCF Plate ($b/a = 2$)			
	The Rayleigh-Ritz method based on Mindlin plate theory ($h/a = 0.001$) [Karunasena and Kitipornchai, 1997]							
	9.214	18.156	26.491	29.184	1.465	3.009	4.989	5.435
	The superposition method [Gorman, 1989]							
	9.139	18.108	26.319	29.083	1.450	2.984	4.955	5.408
	DQFEM based on thin plate theory							
10	9.186	18.070	26.291	29.150	1.466	3.009	4.989	5.424
12	9.205	18.122	26.425	29.163	1.465	3.009	4.989	5.429
14	9.211	18.141	26.466	29.164	1.465	3.009	4.989	5.432
16	9.213	18.149	26.479	29.163	1.465	3.009	4.989	5.433
18	9.214	18.153	26.485	29.162	1.465	3.009	4.989	5.434
20	9.214	18.155	26.487	29.161	1.465	3.009	4.989	5.434

clamped circular plates, respectively. The DQFEM results are in agreement with all the results used for comparisons [Liu and Lee, 2000 and So and Leissa, 1998 for free circular plates; Zhou *et al.*, 2003 and Leissa, 1969 for clamped circular plate], to at least three significant digits.

Table 4 presents comparison studies of bending moments in an elliptical plate (see Fig. 4) with built in and simply supported edges subjected to uniformly

Table 3. Frequencies $\Omega = \omega R \sqrt{\rho/G}$ for 3-D free vibrations of clamped and free circular plates.

h/R	Grid points $M_\xi \times N_\eta \times L_z$	Mode sequence number					
		1	2	3	4	5	6
Completely free circular plates							
0.1	$9 \times 9 \times 4$	0.2576	0.4329	0.5896	0.9655	1.017	1.544
	$11 \times 11 \times 5$	0.2576	0.4329	0.5891	0.9631	1.016	1.530
	$13 \times 13 \times 6$	0.2576	0.4329	0.5891	0.9631	1.016	1.529
	$14 \times 14 \times 7$	0.2576	0.4329	0.5891	0.9631	1.016	1.529
	Ref. b	0.2576	0.4329	0.5892	0.9633	1.017	1.529
	Ref. c	0.2576	0.4329	0.5891	0.9631	1.016	1.529
0.2	$9 \times 9 \times 4$	0.4996	0.8315	1.1069	1.765	1.844	2.689
	$11 \times 11 \times 5$	0.4995	0.8314	1.106	1.762	1.843	2.674
	$13 \times 13 \times 6$	0.4995	0.8314	1.106	1.762	1.843	2.673
	$14 \times 14 \times 7$	0.4995	0.8314	1.106	1.762	1.843	2.673
	Ref. b	0.4997	0.8316	1.107	1.763	1.844	2.677
	Ref. c	0.4995	0.8314	1.106	1.762	1.843	2.673
Clamped circular plates							
0.01	$11 \times 11 \times 3$	0.05003	0.1041	0.1707	0.1948	0.2510	0.3038
	$13 \times 13 \times 4$	0.04997	0.1040	0.1703	0.1944	0.2495	0.2979
	$15 \times 15 \times 5$	0.04993	0.1039	0.1703	0.1943	0.2492	0.2970
	$17 \times 17 \times 6$	0.04991	0.1038	0.1702	0.1942	0.2491	0.2969
	Ref. d	0.04990	0.1038	0.1703	0.1941	0.2490	0.2968
	Ref. e	0.04985	0.1037	0.1702	0.1941	0.2490	0.2968

Ref. b: [Liu and Lee, 2000]; Ref. c: [So and Leissa, 1998]; Ref. d: [Zhou *et al.*, 2003]; Ref. e: [Leissa, 1969].

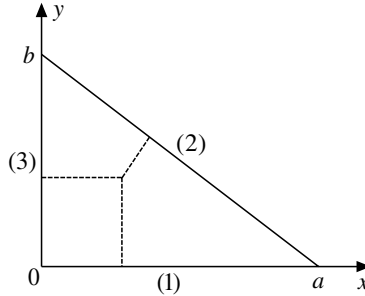


Fig. 3. A triangular plate.

distributed loads. The geometric and material parameters used in the calculation are: $a = 0.50$ (m), $b = 0.33333$ (m), $h = 0.01$ (m), $E = 1$ (MPa), $q = 1.0$ (Pa). Results at points O , A and B as shown in Fig. 4 are presented for which both exact results [Timoshenko and Krieger, 1959] and p -type FEM results [Muhammad and Singh, 2004] are available. The DQFEM solutions based on both the thin plate theory and the Mindlin plate theory are given. Excellent agreements among the three sets of results are found for both clamped and simply supported conditions.

Table 4. Bending moments in an elliptical plate with built in and simply supported edges subjected to uniformly distributed loads.

$M_\xi = N_\eta$	$100(w_0)$	$100(M_x)_0$	$100(M_y)_0$	$100(M_x)_a$	$100(M_y)_b$	$100(w_0)$	$100(M_x)_0$	$100(M_y)_0$
	Clamped boundary conditions				Simply supported boundary conditions			
	Exact solution [Timoshenko and Krieger, 1959]							
	-0.3759	-0.9227	-1.4048	1.1016	2.4791	-1.5549	-2.4662	-3.5660
	p-type FEM solution based Mindlin plate theory [Muhammad and Singh, 2004]							
	-0.3776	-0.9238	-1.4064	1.1012	2.5005	-1.5546	-2.4100	-3.5065
	DQFEM solution based Mindlin plate theory							
7	-0.3765	-0.9210	-1.4014	1.0936	2.4575	-1.5604	-2.4332	-3.5919
9	-0.3773	-0.9231	-1.4047	1.1029	2.4772	-1.5510	-2.4239	-3.5698
11	-0.3773	-0.9231	-1.4048	1.1030	2.4781	-1.5481	-2.4213	-3.5625
13	-0.3773	-0.9232	-1.4048	1.1034	2.4781	-1.5470	-2.4203	-3.5598
15	-0.3773	-0.9232	-1.4048	1.1031	2.4780	-1.5465	-2.4197	-3.5587
17	-0.3773	-0.9232	-1.4048	1.1034	2.4779	-1.5462	-2.4195	-3.5583
	DQFEM solution based thin plate theory							
7	-0.3753	-0.9207	-1.4016	1.0919	2.4575	-1.5437	-2.4189	-3.5552
9	-0.3760	-0.9226	-1.4048	1.1010	2.4774	-1.5446	-2.4195	-3.5576
11	-0.3760	-0.9227	-1.4048	1.1013	2.4792	-1.5447	-2.4192	-3.5572
13	-0.3760	-0.9227	-1.4049	1.1012	2.4784	-1.5447	-2.4187	-3.5564
15	-0.3760	-0.9228	-1.4049	1.1013	2.4788	-1.5446	-2.4180	-3.5554

Table 5. Convergence study of frequency parameters $\Omega = \omega b^2 \sqrt{\rho h/D}$ for rectangular plates with mixed edge supports ($a_1/a = 0.375$).

Case	$N_\xi = N_\eta$	Mode sequence					
		1	2	3	4	5	6
1	13	23.25	50.73	57.31	82.84	99.15	110.4
	14	23.24	50.71	57.28	82.79	99.14	110.3
	15	23.23	50.70	57.26	82.75	99.13	110.3
	16	23.23	50.69	57.24	82.71	99.12	110.2
	Ref. f	23.23	50.69	57.25	82.73	99.12	110.3
2	13	27.82	52.34	66.10	87.03	99.63	123.1
	14	27.80	52.31	66.01	86.87	99.61	123.1
	15	27.77	52.27	65.97	86.81	99.58	122.9
	16	27.76	52.25	65.91	86.71	99.57	122.9
	Ref. f	27.77	52.26	65.93	86.75	99.57	122.9
3	13	13.13	17.15	37.27	44.79	48.34	74.05
	14	13.11	17.13	37.26	44.76	48.31	74.05
	15	13.10	17.12	37.26	44.73	48.28	74.05
	16	13.09	17.11	37.26	44.71	48.26	74.05
	Ref. f	13.10	17.12	37.26	44.73	48.28	74.06

Ref. f: [Su and Xiang, 2002].

For a thin plate with mixed support conditions or discontinuous boundaries, as shown in Fig. 5, the first six frequencies of DQFEM using three elements coincide well, as shown in Table 5, with those of [Su and Xiang, 2002] using a novel domain decomposition method. It follows that DQFEM can be used conveniently to cope with complex problems as FEM.

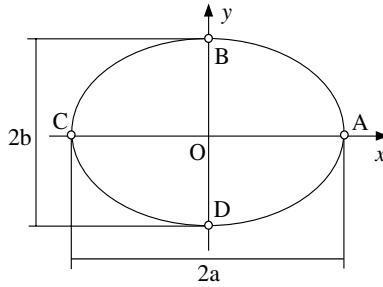


Fig. 4. An elliptic plate.

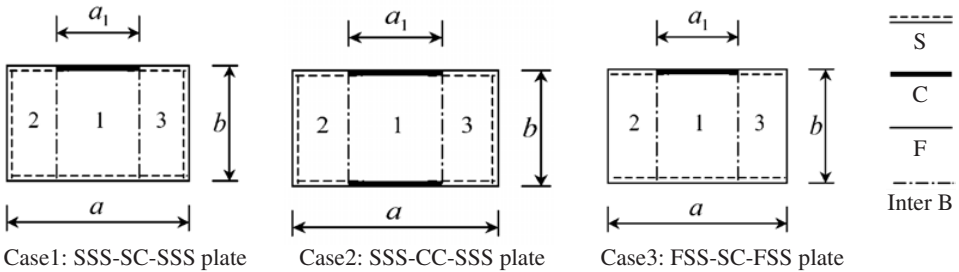


Fig. 5. Rectangular plates with discontinuous boundaries.

5. Conclusion

A differential quadrature finite element method (DQFEM) was studied systematically and applied successfully to 1-D to 3-D static and dynamic structural problems, and the free vibrations of plane problem, the static problems of Kirchhoff and Mindlin plates, the 3-D elasticity problems were investigated for the first time using DQFEM which can be viewed as a new methodology of formulating finite element method. DQFEM has incorporated the high accuracy and efficiency of DQM, especially for formulating high order elements, and the simplicity of imposing boundary conditions, the symmetry of element matrices of FEM.

The DQ rules were reformulated and its efficient implementation presented here is significant to the practical application of DQFEM, from whose explicit formulations of different elements one can concluded that DQFEM can be used simply in the same way as FEM. Moreover, the DQFE matrices are compact and well conditioned, and the mass matrices for C^0 continuity problems are diagonal, which can reduce the computational cost of dynamic problems. Numerical comparison studies with results available in literature were carried out for free vibration of 2-D and 3-D plates and bending of thin and Mindlin plates with arbitrary shapes, which validate the high accuracy and rapid convergence of DQFEM.

Acknowledgements

The authors gratefully acknowledge the support from the National Natural Science Foundation of China (Grant No. 10772014).

References

- Atkatsch, R. S., Baron, M. L. and Bieniek, M. P. [1980] "A finite difference variational method for bending of plates," *Computers and Structures* **11**, 573–577.
- Babuska, Szabo, B. and Katz, I. N. [1981] "The p -version of the finite element method," *SIAM Journal on Numerical Analysis* **18**(3), 515–541.
- Bardell, N. S. [1996] "An engineering application of the h - p Version of the finite element method to the static analysis of a Euler-Bernoulli beam," *Computers & Structures* **59**(2), 195–211.
- Bardell, N. S., Langley, R. S. and Dunsdon, J. M. [1996] "On the free in-plane vibration of isotropic rectangular plates," *Journal of Sound and Vibration* **191**(3), 459–467.
- Barve, V. D. and Dey, S. S. [1990] "Isoparametric finite difference energy method for plate bending problems," *Computers and Structures* **17**, 459–465.
- Bellman, R. and Casti, J. [1971] "Differential quadrature and long term integration," *Journal of Mathematical Analysis and Applications* **34**, 235–238.
- Bert, C. W., Jang, S. K. and Striz, A. G. [1988] "Two new approximate methods for analyzing free vibration of structural components," *AIAA Journal* **26**, 612–618.
- Bert, C. W. and Malik, M. [1996] "Differential quadrature method in computational mechanics: A review," *Applied Mechanics Reviews* **49**, 1–28.
- Bert, C. W. and Malik, M. [1996] "The differential quadrature method for irregular domains and application to plate vibration," *International Journal of Mechanical Sciences* **38**, 589–606.
- Brush, D. O. and Almroth, B. O. [1975] *Buckling of Bars, Plates and Shells* (McGraw-Hill, New York).
- Bushnell, D. [1973] "Finite difference energy models versus finite element models: two variational approaches in one computer program," in *Numerical and Computer Methods in Structural Mechanics*, ed. S. J. Fenves, N. Perrone, J. Robinson, W. C. Schnobrich (Academic Press, New York).
- Campion, S. D. and Jarvis, J. L. [1996] "An investigation of the implementation of the p -version finite element method," *Finite Elements in Analysis and Design* **23**, 1–21.
- Chen and New, C. [1999] "A differential quadrature finite element method. Applied mechanics in the Americas," *Proceedings of the 6th Pan-American Congress of Applied Mechanics and 8th International Conference on Dynamic Problems in Mechanics*, PACAM VI, Rio de Janeiro, Brazil; US; 4–8 Jan., pp. 305–308.
- Demkowicz, L., Oden, J. T., Rachowicz, W. and Hardy, O. [1989] "Toward a universal h - p adaptive finite element strategy, Part 1: Constrained approximation and data structure," *Computer Methods in Applied Mechanics and Engineering* **77**, 79–112.
- Duan, M., Miyamoto, Y., Iwasaki, S. and Deto, H. [1999] "5-node hybrid/mixed finite element for Reissner-Mindlin plate," *Finite Elements in Analysis and Design* **33**, 167–185.
- Fielding, L. M., Villaca, S. F. and Garcia, L. F. T. [1997] "Energetic finite differences with arbitrary meshes applied to plate bending problems," *Applied Mathematical Modelling* **21**, 691–698.
- Gorman, D. J. [1983] "A highly accurate analytical solution for free vibration analysis of simply supported right triangular plates," *Journal of Sound and Vibration* **89**(1), 107–118.

- Gorman, D. J. [1986] “Free vibration analysis of right triangular plates with combinations of clamped-simply supported boundary conditions,” *Journal of Sound and Vibration* **106**(3), 419–431.
- Gorman, D. J. [1989] “Accurate free vibration analysis of right triangular plates with one free edge,” *Journal of Sound and Vibration* **131**(1), 115–125.
- Griffin, D. S. and Varga, R. S. [1963] “Numerical solution of plane elasticity problems,” *Journal of the Society for Industrial Applied Mathematics* **11**, 1046–1060.
- Haghighi, M. R. G., Eghtesad, M. and Malekzadeh, P. [2008] “Coupled DQ–FE methods for two dimensional transient heat transfer analysis of functionally graded material,” *Energy Conversion and Management* **49**, 995–1001.
- Houbolt, J. C. [1958] “A Study of Several Aerothermoelastic Problems of Aircraft Structure in High-speed Flight,” (Verlag Leemann, Zurich).
- Karunasena, W. and Kitipornchai, S. [1997] “Free vibration of shear-deformable general triangular plates,” *Journal of Sound and Vibration* **199**(4), 595–613.
- Leissa, A. W. [1969] “Vibration of Plates,” NASA SP-160. Office of Technology Utilization, Washington, DC.
- Liu, C. F. and Lee, Y. T. [2000] “Finite element analysis of three-dimensional vibrations of thick circular and annular plates,” *Journal of Sound and Vibration* **233**(1), 63–80.
- Malik, M. and Bert, C. W. [2000] “Vibration analysis of plates with curvilinear quadrilateral planforms by DQM using blending functions,” *Journal of Sound and vibration* **230**, 949–954.
- Muhammad, T. and Singh, A. V. [2004] “A p-type solution for the bending of rectangular, circular, elliptic and skew plates,” *International Journal of Solids and Structures* **41**, 3977–3997.
- Oden, J. T. and Demkowicz, L. [1991] “*h-p* adaptive finite element methods in computational fluid dynamics,” *Computer Methods in Applied Mechanics and Engineering* **89**, 11–40.
- Rong, T. Y. and Lu, A. Q. [2003] “Generalized mixed variational principles and solutions of ill-conditioned problems in computational mechanics. Part II: Shear locking,” *Computer Methods in Applied Mechanics and Engineering* **192**, 4981–5000.
- Satyamurthy, K., Khot, N. S. and Bauld, N. R. [1980] “An automated, energy-based finite difference procedure for the elastic collapse of rectangular plates and panels,” *Computers and Structures* **11**, 239–249.
- Shephard, M. S., Dey, S. and Flaherty, J. E. [1997] “A straightforward structure to construct shape functions for variable *p*-order meshes,” *Computer Methods in Applied Mechanics and Engineering* **147**, 209–233.
- Shu, C. [2000] *Differential Quadrature and its Application in Engineering* (Springer-Verlag, London).
- Singh, J. P. and Dey, S. S. [1990] “Variational finite difference method for free vibration of sector plates,” *Journal of Sound and Vibration* **136**, 91–104.
- So, J. and Leissa, A. W. [1998] “Three-dimensional vibrations of thick circular and annular plates,” *Journal of Sound and Vibration* **209**, 15–41.
- Striz, A. G., Chen, W. and Bert, C. W. [1994] “Static analysis of structures by the quadrature element method (QEM),” *International Journal of Solids and Structures* **31**, 2807–2818.
- Striz, A. G., Chen, W. L. and Bert, C. W. [1995] “High accuracy plane stress and plate elements in the quadrature element method,” *Proceedings of the 36th AIAA/ASME/ASCE/AHS/ASC*, pp. 957–965.
- Striz, A. G., Chen, W. L. and Bert, C. W. [1997] “Free vibration of plates by the high accuracy quadrature element method,” *Journal of Sound and Vibration* **202**, 689–702.

- Su, G. H. and Xiang, Y. [2002]. "A non-discrete approach for analysis of plates with multiple subdomains," *Engineering Structures* **24**, 563–575.
- Timoshenko, S. and Krieger, S. W. [1959] *Theory of Plates and Shells* (McGraw Hill Book Co, NY).
- Xing, Y. F. and Liu, B. [2009] "High-accuracy differential quadrature finite element method and its application to free vibrations of thin plate with curvilinear domain," *Int. J. Numer. Meth. Engng* (2009), DOI: 10.1002/nme.2685.
- Zhou, D., Au, F. T. K., Cheung, Y. K. and Lo, S. H. [2003] "Three-dimensional vibration analysis of circular and annular plates via the Chebyshev–Ritz method," *International Journal of Solids and Structures* **40**, 3089–3105.
- Zhong, H. and He, Y. [1998] "Solution of Poisson and Laplace equations by quadrilateral quadrature element," *International Journal of Solids and Structures* **35**, 2805–2819.
- Zhong, H. and Yu, T. [2009] "A weak form quadrature element method for plane elasticity problems," *Appl. Math. Modell.* doi:10.1016/j.apm.2008.12.007.